CHAPTER 3

3. MATHEMATICAL MODELING AND PID CONTROLLER DESIGN TECHNIQUES

This chapter is divided into three sections. The first section deal with modeling of Continuous Stirred Tank Reactor (CSTR) and designing of PI controller based on FOPDT equivalent of CSTR using PI tuning techniques given by SIMC [46] and Astrom and Hagglund [20] to control the output concentration of CSTR. A PI controller based on second-order transfer function model was also designed by using a computational optimization method to control the outlet concentration of CSTR. The second section deals with the PID controller design using the Direct Synthesis (DS) method for stable second-order time delay process models, and finally, the third part of this chapter discussed the IMC-PID controller design for unstable second-order time delay transfer functions.

3.1 Mathematical Modeling

Mathematical modeling is used to develop the transfer function of the processes and which is further used to design PI/PID controller for controlling the process variable viz. output concentration in CSTR and temperature of fermenter for production of ethanol. The mathematical models of the process can be developed using mass and energy balance approach. These models can be used as an alternative to the real processes for the controller tuning, performance evaluation, optimizing the plant operation, and handle the critical safety issue without disturbing the real process [25]. A new control scheme can be

developed with the help of the dynamics response of the process model and applied to the real processes without affecting the plant operation.

3.1.1 Modeling of Continuous Stirred Tank Reactor (CSTR)

Controlling the output parameter in CSTR is a challenging problem from a control point of view because of its nonlinear behavior and keeping this fact in mind one of the objectives of present work is to evaluate the performance of available PI/PID tuning techniques for control of output concentration of a CSTR which exhibit non-linear behavior. As conventional PID design and tuning techniques are mostly based on linear models. The nonlinear models are first linearized, and then tuning parameters are calculated. The PID controller designed using above approach work well in linear and slightly non-linear stable processes. The performance of a PID controller may not be up to the mark applied to a real process having significant nonlinearity and unstable characteristics. To overcome this problem in this study, the tuning approach was also tested on a mathematical model of the process as close as possible to the real process. The study will help us to evaluate the efficacy of linear model-based PID design on the nonlinear process.

In order to control CSTR, the controller design methods developed by Astrom and Hagglund [20], SIMC [46], and computational optimization method [84] were used to design and tune the controller. The performance of the designed controller was tested on a linearized model as well as nonlinear models that are closer to a real system. The computational optimization method was used to design an optimal PI controller for a second-order transfer function using MATLAB program [84]. In this technique, different constraints such as maximum overshoot, settling time, and rise time may be imposed to achieve better control performance in the designing of PI/PID controller for a first or

second-order models. In the present case, a PI controller was designed with a constraint of overshoot less than 20 % of the ultimate value. Two other methods developed by SIMC [46] and Astrom and Hagglund [20] for PI tuning based on FOPDT model were also used to control the output concentration of CSTR.

A CSTR in which a first-order chemical reaction of A → B is taking place was considered to develop its mathematical model, as shown in Fig. 3.1 [85]. The F_i and F_o are input and output flow rate respectively. The temperature inside the reactor is T and the inlet temperature denoted by T_{in}. The outlet concentration of the component is C_A.

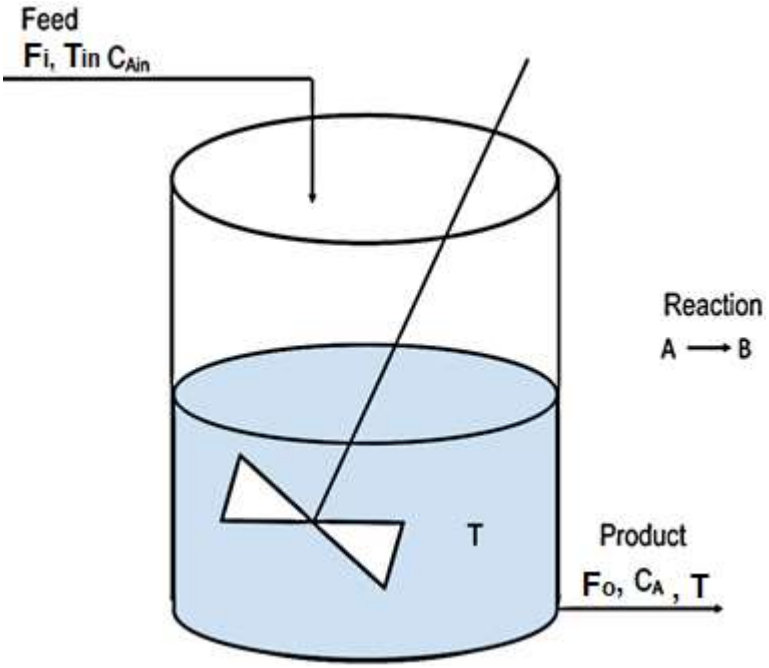

Fig. 3.1 CSTR with a first-order chemical reaction.

The outlet concentration from the reactor is found by solving the different mathematical equations dealing with total mass, component, and energy balance of CSTR. The steady-state condition was considered, therefore the inlet flow rate F_i would be equal to the outlet flow rate, i.e., $F_i = F_o = F$, and thus the total mass balance equation is eliminated. For the

development of the mathematical model of the reactor, the various operating steady-state parameters are shown in Table 3.1.

Table 3.1 Steady-state operating parameter of CSTR [85]

Parameter	**Value**
Reactor volume, V	5 m^3
Outlet concentration of component A, C_A	200.13 kg/m^3
Inlet concentration of component A, C_{Ain}	800 kg/m^3
Total volumetric flow, F	0.005 m^3/s
Pre-exponential constant, k	18.75 s^{-1}
Activation energy for the reaction, E	30 kJ/mol
Reactor temperature, T	413 K
Temperature of inlet flow, Tin	353 K
Density, ρ	800 kg/m^3
Specific heat, c_p	1.0 kJ/kg.K
Heat of reaction (exothermic), ΔH	5.3 kJ/kg
Heat supplied to the reactor, Q	224.1 kJ/sec
Gas constant, R	0.0083 kJ/mol.k

The mathematical equations for the component and energy balance of the reactor were taken from [85] and used in the present work for the control of the outlet concentration of component A.

The mass balance for component A and the energy balance for the reactor can be written as

$$V\frac{dC_A}{dt} = F(C_{Ain} - C_A) - Vke^{-E/RT}C_A \quad (3.1)$$

$$\rho V c_p \frac{dT}{dt} = F\rho c_p (T_{in} - T) + Vke^{-E/RT}C_A \Delta H + Q \quad (3.2)$$

The nonlinear equations (Eq. 3.1 and Eq. 3.2) for component and energy balance were linearized using Taylor's approximation series around steady-state operating parameters as given in Table 3.1 and after that these equations were converted into a second-order transfer function (TF 1) using Laplace Transform as given by Eq. (3.3).

$$TF\ 1 = \frac{C_A(s)}{F_i(s)} = 6.69 \times 10^4 \frac{457.5s+1}{2.55\times10^5 s^2+1255.5s+1} \quad (3.3)$$

The detailed procedure for obtaining the transfer function model has been provided in [85]. The second-order transfer function model of Eq. (3.3) was simplified to a first-order plus dead time (FOPDT) TF 2 model using its dynamic open-loop response for a step change of 5% in the reactor input flow rate F_i.

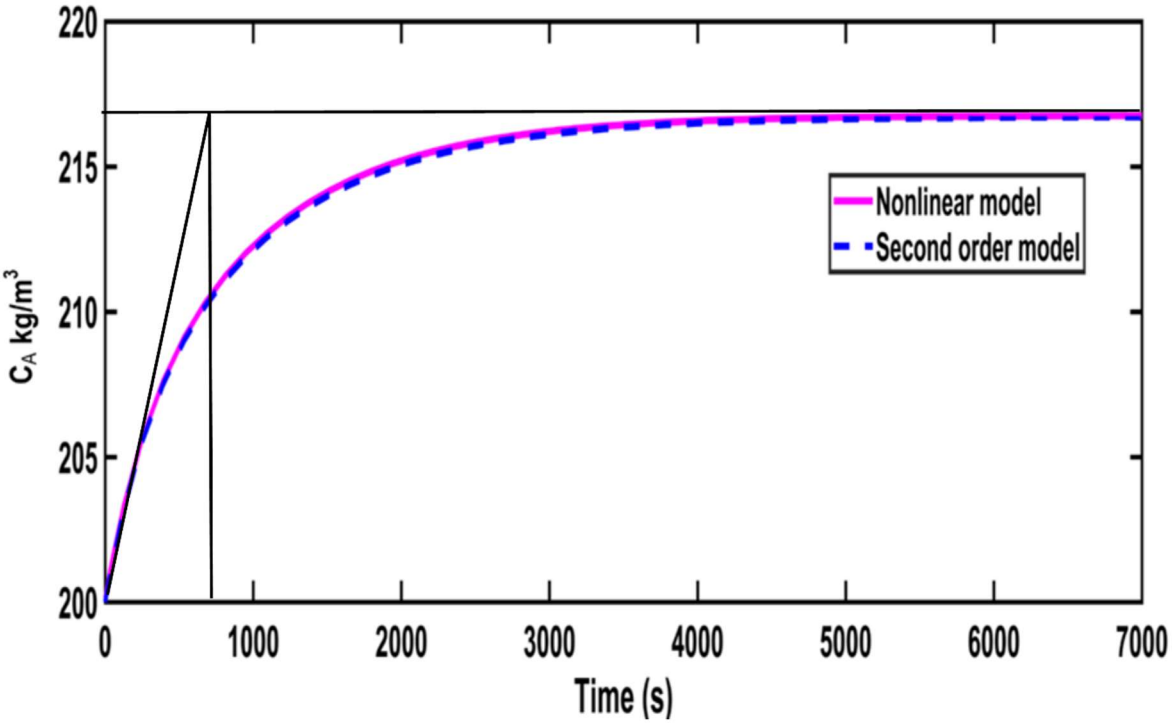

Fig. 3.2 Open-loop response curve using MATLAB/SIMULINK

The open-loop response curve was generated using MATLAB/SIMULINK by introducing a step change of 5 % of the flow rate into set-point, as shown in Fig. 3.2. The process parameters for FOPDT model were calculated using this response curve, and the reduced FOPDT model is given by Eq. (3.4).

$$TF\ 2 = \frac{C_A(s)}{F_i(s)} = \frac{66800}{671s+} e^{-1s} \quad (3.4)$$

The time delay of 1 second was assumed in the process for the designing of a PI controller using various well-known tuning approaches.

3.1.2 Modeling of a bioreactor in fermentation process

A continuous operating bioreactor (fermentor) used for the production of alcohol, as shown in Fig. 3.3 was taken from [69, 70] in the present study. The behavior of the bioreactor was assumed as a continuous stirred tank reactor (CSTR) in which biological reactions are occurring. The mathematical models of the fermentation process for the production of alcohol have been developed and used by various researchers to design the controller and the performance of control-loop was evaluated using different control strategies. Various works of literature are available on the development of mathematical models of the bioreactor and its implementation for temperature control [69, 70]. The biomass production in the reactor is the main factor for the ethanol production rate. The concentration and production of biomass were mainly affected by the dilution rate (Fe/V). Due to the availability of a large number of data for comparison, control of temperature in the bioreactor for ethanol production was taken to evaluate the controller performance.

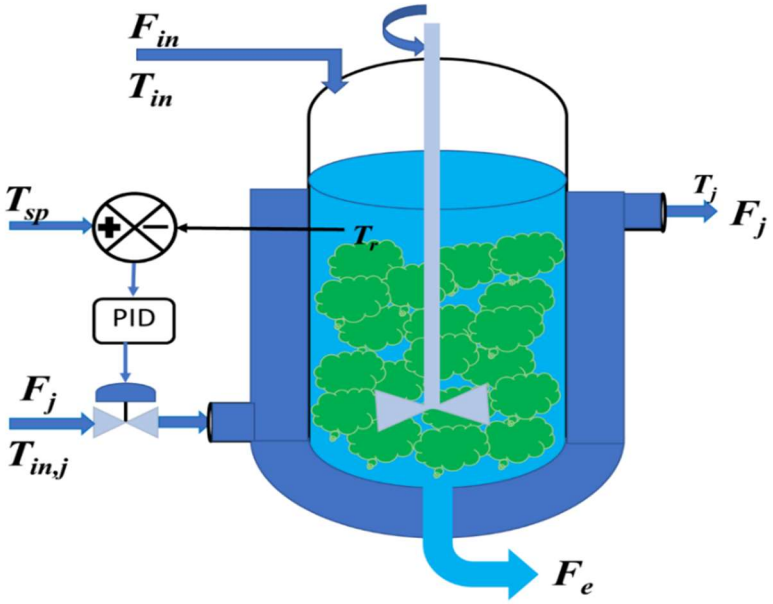

Fig. 3.3 Bioreactor temperature control loop

Figure 3.3 shows the temperature control loop of the continuous bioreactor in which the temperature of the reactor is controlled by manipulating the jacket feed flow rate. The fundamental mathematical model of the bioreactor was developed to study its dynamic behavior, and the model was used for designing of controller.

The following assumptions were taken to simply the behaviour of the bioreactor as CSTR. If the bioreactor follows the below assumptions, its behavior will be close to behavior of CSTR.

- Perfect mixing in the reactor
- Constant stirring speed in the reactor
- pH of the bioreactor is constant

- The substrate feed flow and output flow from the reactor consists of the product are constant
- The input concentrations of biomass and substrate are constant.

The modified Monod equation according to the Michaelis-Menten rate kinetics equilibrium developed by Aiba [86] as given by Eq. (3.5) was used to represent biokinetics in the reactor.

$$\mu = \mu_o \frac{C_s}{K_s + C_s} e^{-K_1 C_p} \tag{3.5}$$

The balance equations representing reactor are as follows:

The total mass balance of the reactor is given by [rate of accumulation of total mass] = [input flow rate] – [output flow rate] and represented by Eq. (3.6)

$$\frac{dv}{dt} = F_i - F_e \tag{3.6}$$

Mass balance of biomass is given by [rate of change of biomass (yeast) concentration] = [production of biomass in fermentation] – [biomass (yeast) leaving the reactor] and represented by Eq. (3.7).

$$\frac{dC_x}{dt} = \mu_x C_x \frac{C_s}{K_s + C_s} e^{-K_p C_p} - \frac{F_e}{V} C_x \tag{3.7}$$

Mass balance for product ethanol is given by [rate of change of product (ethanol) concentration] = [production of ethanol in fermentation reaction]−[product (ethanol) leaving the reaction] and represented by Eq. (3.8).

$$\frac{dC_p}{dt} = \mu_p C_x \frac{C_s}{K_{s1} + C_s} e^{-K_{p1} C_p} - \frac{F_e}{V} C_p \tag{3.8}$$

Mass balance for substrate (glucose) is given by [rate of change of substrate] = − [substrate consumed by biomass for growth] − [substrate consumed by biomass for ethanol production] + [glucose supplied by feed] − [glucose leaving the reaction] and represented by Eq. (3.9).

$$\frac{dC_s}{dt} = -\frac{1}{R_{sx}}\mu_x C_x \frac{C_s e^{-K_p C_p}}{K_s + C_s} - \frac{1}{R_{sp}}\mu_p C_x \frac{C_s e^{-K_p C_p}}{K_{s1} + C_s} + \frac{F_{in}}{V} C_{s,in} - \frac{F_e}{V} C_s \tag{3.9}$$

Energy balance for reactor

For the growth of cells or ethanol the production in the fermentation process, the temperature of the bioreactor, and jacket are essential parameters to consider since there is a certain temperature range for the growth of particular microorganisms [87]. Hence, the mathematical model of energy balance for jacket and reactor must be included to improve the real-time performance of the process. The balanced equation representing the energy balance for the jacket and the reactor is given as follows:

The energy balance for a reaction is given by [Heat accumulated in reactor] = [Heat at inlet] – [Heat at outlet] + [Heat generated from reaction] – [Heat transferred to the jacketed] and represented by Eq. (3.10).

$$\frac{dT_r}{dt} = \frac{F_{in}}{V}(T_{in} + 273) - \frac{F_e}{V}(T_r + 273) + \frac{r_{o_2}\Delta H_r}{32\rho_r C_{heat,r}} - \frac{K_T A_T (T_r - T_{in,j})}{V\rho_r C_{heat,r}} \tag{3.10}$$

Energy balance for a jacket is given by [Heat accumulated in jacket] = [Heat at coolant inlet] + [Heat at coolant outlet] and represented by Eq. (3.11).

$$\frac{dT_j}{dt} = \frac{F_j}{V_j}\left(T_{in,j} - T_j\right) + \frac{K_T A_T (T_r - T_j)}{V_j \rho_j C_{heat,j}} \tag{3.11}$$

Mass balance for dissolved oxygen concentration (C_{o_2}) is given by [concentration of dissolved oxygen in the substrate during reaction] = [concentration of oxygen dissolved in inlet feed supplied to the reactor] – [consumption of oxygen in fermentation reactions] and represented by Eq. (3.12).

$$\frac{dC_{o_2}}{dt} = K_L a\left(C_{o_2}^* - C_{o_2}\right) - r_{o_2} - \frac{F_e}{V} C_{o_2} \tag{3.12}$$

The growth of cell is affected by the concentration of dissolved oxygen (C_{o_2}) in the bioreactor for the fermentation process. The dissolved oxygen helps to grow the cells at a faster rate and increases cell density and ultimately increases oxygen consumption. Thus, the dissolved oxygen level decreases and therefore required external oxygen supply to maintain the desired dissolved oxygen level [88]. The biomass overgrows in the presence of excess dissolved oxygen, and ultimately the ethanol production rate decreases. Therefore, the dissolved oxygen should maintain at some optimum level to achieve the maximum production rate of ethanol [89]. The pH of the reactor is another critical parameter that affects the operation of the bioprocess. The following models of the bioreactor are used for the control of dissolved oxygen concertation and pH.

The liquid phase equilibrium concentration of oxygen is written as

$$C_{o_2}^* = (14.16 - 0.3943T_r + 0.007714T_r^2 - 0.0000646T_r^3)10^{-\sum H_i I_i} \tag{3.13}$$

The global effect of ionic strengths is given as follows

$$\sum H_i I_i = 0.5H_{Na}\frac{m_{NaCl}}{M_{NaCl}}\frac{M_{Na}}{V} + 2H_{Ca}\frac{m_{CaCO_3}}{M_{CaCO_3}}\frac{M_{Ca}}{V} + 2H_{Mg}\frac{m_{MgCl_2}}{M_{MgCl_2}}\frac{M_{Mg}}{V} + 0.5H_{Cl}\left(\frac{m_{NaCl}}{M_{NaCl}} + 2\frac{m_{MgCl_2}}{M_{MgCl_2}}\right)\frac{M_{Cl}}{V} + 2H_{CO_3}\frac{m_{CaCO_3}}{M_{CaCO_3}}\frac{M_{CO_3}}{V} + 0.5H_H 10^{-pH} + 0.5H_{OH}10^{-(14-p\ )} \tag{3.14}$$

$$K_L a = K_L a_0 \cdot 1.024^{(T_r - 20)} \tag{3.15}$$

$$r_{O_2} = \mu_{O_2} \frac{1}{Y_{O_2}} C_x \frac{C_{O_2}}{K_{O_2} + C_{O_2}} \cdot 1000 \tag{3.16}$$

$$\mu_x = A_1 e^{\left[-\frac{E_{a1}}{R(T_r+273)}\right]} - A_2 e^{\left[-\frac{E_{a2}}{R(T_r+273)}\right]} \tag{3.17}$$

The bioreactor model parameters and steady-state operating parameters are given in Table 3.2 and Table 3.3 [70] which were used to obtain the open-loop response curves for various operating parameters. The open-loop response curves for different process parameters were obtained by simulating the mathematical models represented by Eq. 3.5 - Eq. 3.17 using the SIMULINK toolbox of MATLAB and shown in Fig. 3.4 to Fig. 3.9.

Table 3.2 Bioreactor model parameters

$A_1 = 9.5 \times 10^8$	$H_{Na} = -0.55$	$\rho_r = 1080\ g\ L^{-1}$
$A_2 = 2.55 \times 10^{33}$	$K_L a_0 = 38\ h^{-1}$	$m_{NaCl} = 500\ g$
$A_T = 1\ m^2$	$K_{O_2} = 8.886 mg L^{-1}$	$m_{CaCO_3} = 100\ g$
$C_{heat,ag} = 4.18\ J g^{-1} K^{-1}$	$K_p = 0.139 g L^{-1}$	$m_{MgCl_2} = 100\ g$
$C_{heat,r} = 4.18\ J g^{-1} K^{-1}$	$K_{p1} = 0.07 g L^{-1}$	$R = 8.31\ J mol^{-1} K^{-1}$
$E_{a1} = 55000\ J mol^{-1}$	$K_S = 1.03\ g L^{-1}$	$M_{Na} = 23\ g\ mol^{-1}$
$E_{a2} = 22000\ J mol^{-1}$	$K_{S1} = 1.68\ g L^{-1}$	$M_{Ca} = 40\ g\ mol^{-1}$
$H_{OH} = 0.941$	$K_T = 3.6 \times 10^5 J\ h^{-1} m^{-2} K^{-1}$	$M_{Mg} = 24\ g\ mol^{-1}$
$H_H = -0.774$	$R_{SP} = 0.435$	$M_{Cl} = 35.5\ g\ mol^{-1}$
$H_{CO_3} = 0.485$	$R_{Sx} = 0.607$	$M_{CO_3} = 60 g\ mol^{-1}$
$H_{Cl} = 0.844$	$Y_{O_2} = 0.970\ mg\ mg^{-1}$	$\mu_P = 1.79\ h^{-1}$
$H_{Mg} = -0.314$	$\Delta Hr = 518 kJ\ mol^{-1}\ O_2$	$\rho_u = 1000 g L^{-1}$
$H_{Ca} = -0.303$	$\mu_{O_2} = 0.5\ h^{-1}$	

Table 3.3 Steady-state operating parameters [72]

Parameter	Description	Values	Nominal operating conditions
F_i	Input Flow	51 $l\ h^{-1}$	$F_i = F_e = 51l\ h^{-1}$
F_e	Output Flow	51 $l\ h^{-1}$	$F_j = 18\ Lh^{-1}$
T_{in}	Inlet flow temperature	25 °C	$T_{in} = 25$ °C
$T_{in,j}$	Temperature of input Cooling agent	15 °C	$T_{in,j} = 15$ °C, $T_r = 29.5732$ °C
$C_{s,in}$	Concentration of Glucose input Flow	60 g/l	T_j=27.0539 °C $C_{s,in} = 60\ g/l$
V	Total volume of the reaction medium	1000 l	$C_s = 29.7389\ g/l$,
V_j	Volume of the jacket	50 l	$C_P = 12.5152\ g/l$
pH	Potential of hydrogen	6	$C_{O2} = 3.107\ mg/l$, $C_X = 0.904677 g/l$
F_j	Flow rate of cooling agent	18 $l\ h^{-1}$	$V = 1000\ l$
$K_L a$	Mass Transfer Coefficient for oxygen	$38(1024)^{T_r-20}$	$pH = 6$

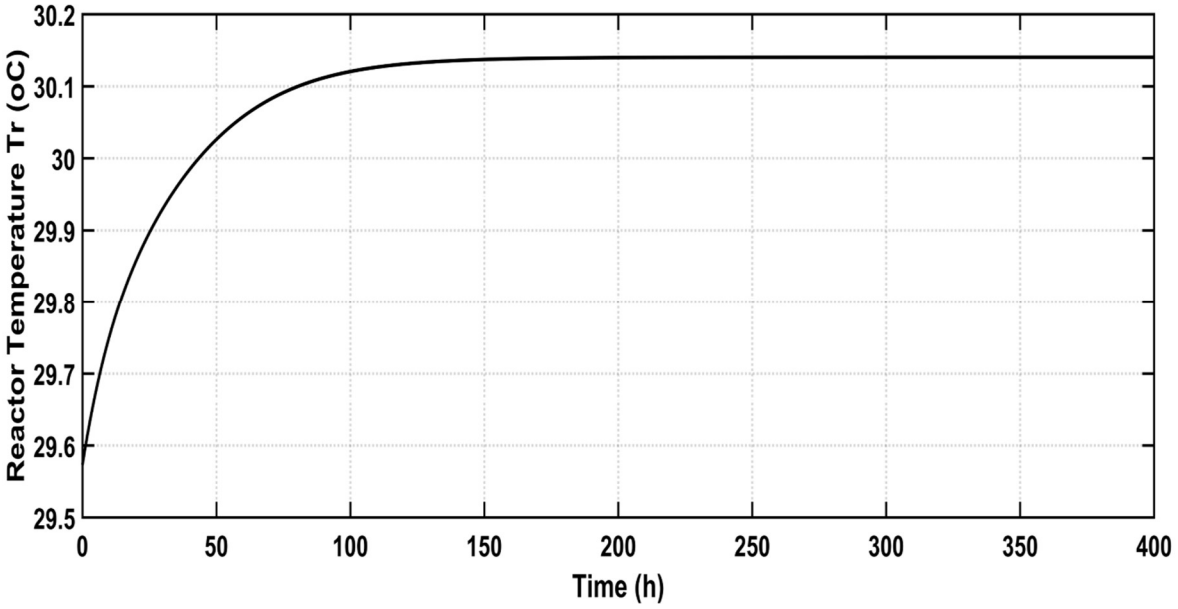

Fig. 3.4 Open-loop response for bioreactor temperature.

Figure 3.4 and Fig. 3.5 show the open-loop response of reactor and jacket temperatures at nominal operating conditions which were taken from [72] and given in Table 3.3. The dynamics of the bioreactor was very slow and temperature of reactor increses slightly due

to biochemical reaction occurring. The corresponding jacket temperature Tj is shown in Fig. 3.5. The product concentration *C*p of ethanol also increses and finally gets steady-state as increase in temperature of the reactor as shown in Fig. 3.6.

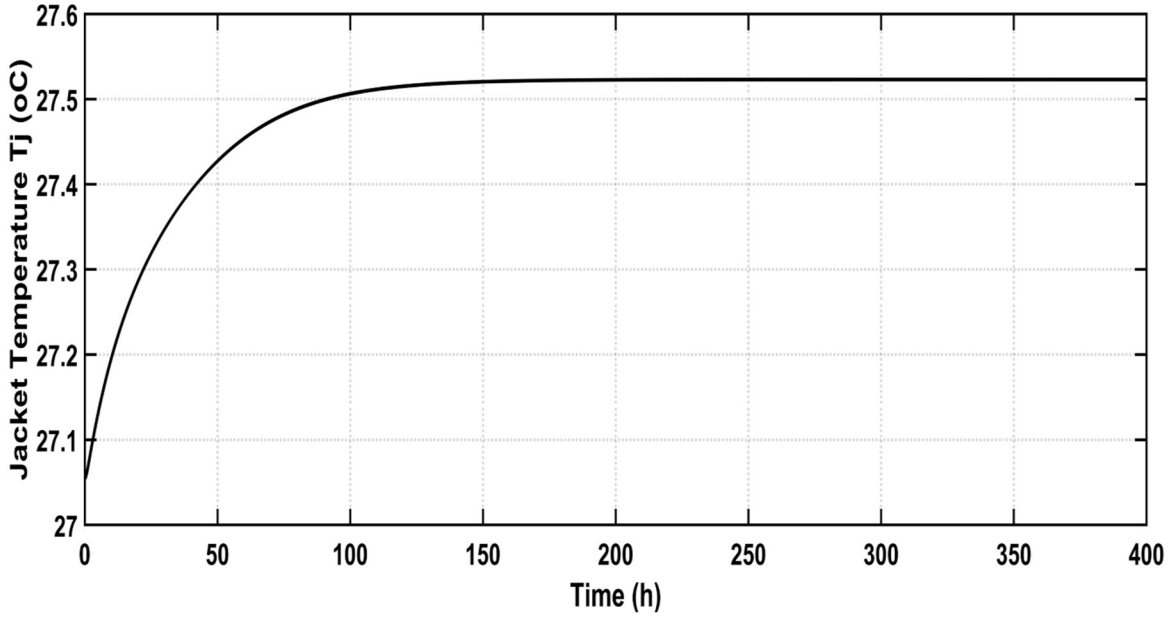

Fig. 3.5 Open-loop response for jacket temperature.

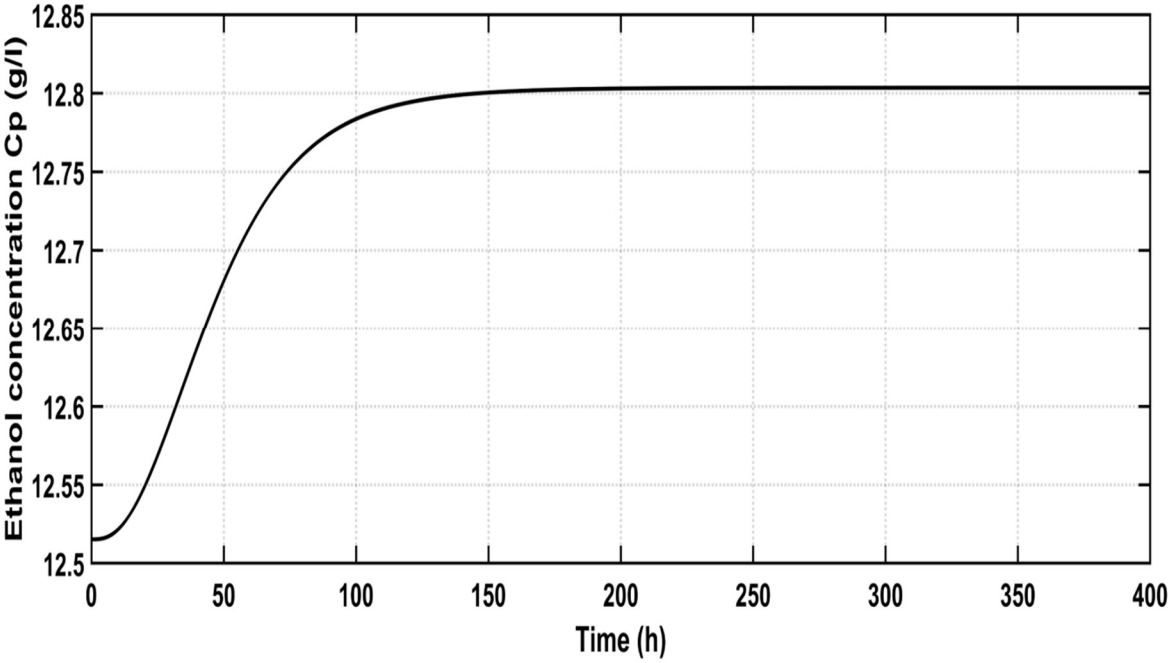

Fig. 3.6 Open-loop response for Ethanol concentration.

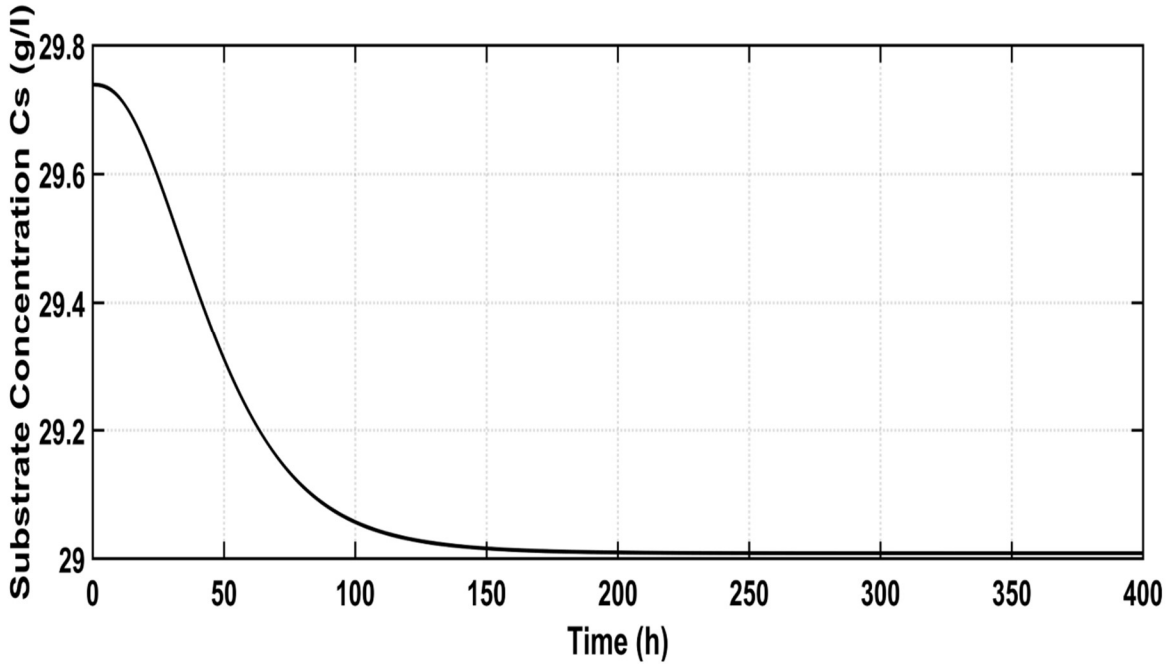

Fig. 3.7 Open-loop response for substrate concentration.

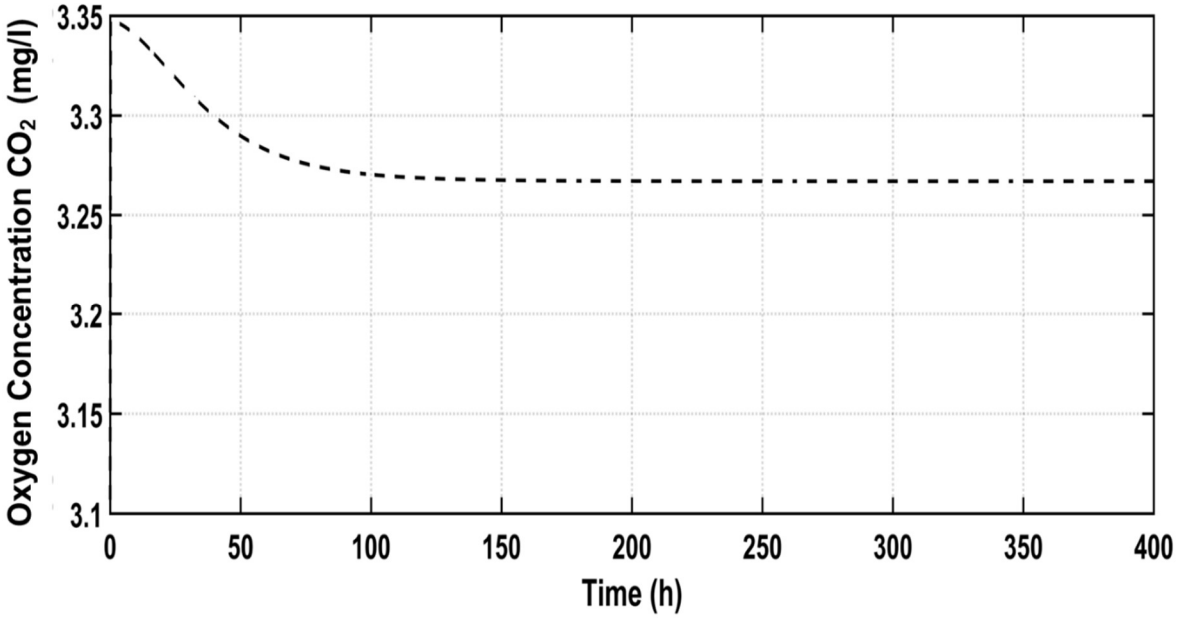

Fig. 3.8 Open-loop response for dissolved oxygen concentration.

The substrate concentration Cs and dissolved concentration C_{O2} are decreases as temperature of the reactor increses as shown in Fig. 3.7 and 3.8 respectively. As the temperature of reactor is incresed, more substrate was converted to product Cp. Therefore,

the substrate concentration Cs decreses. As the biochemical reaction proceeds the biomass concentration Cx also increses as shown in Fig. 3.9. The biomass concentration Cx increses more biochemical reaction takes and consequently temperature of the reactor increses.

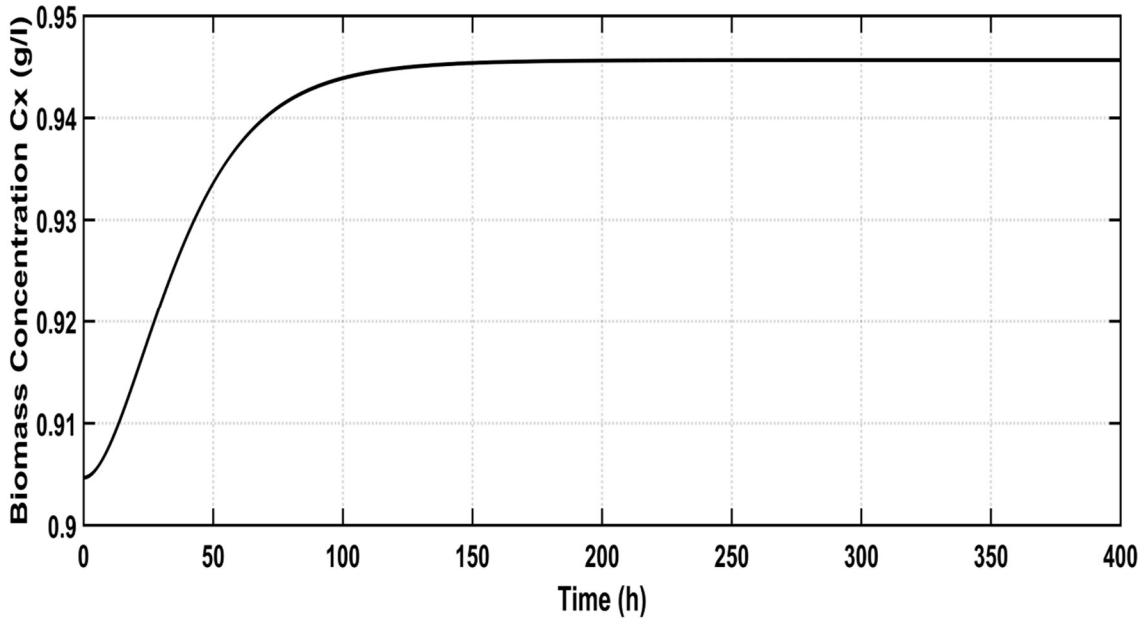

Fig. 3.9 Open-loop response for biomass concentration

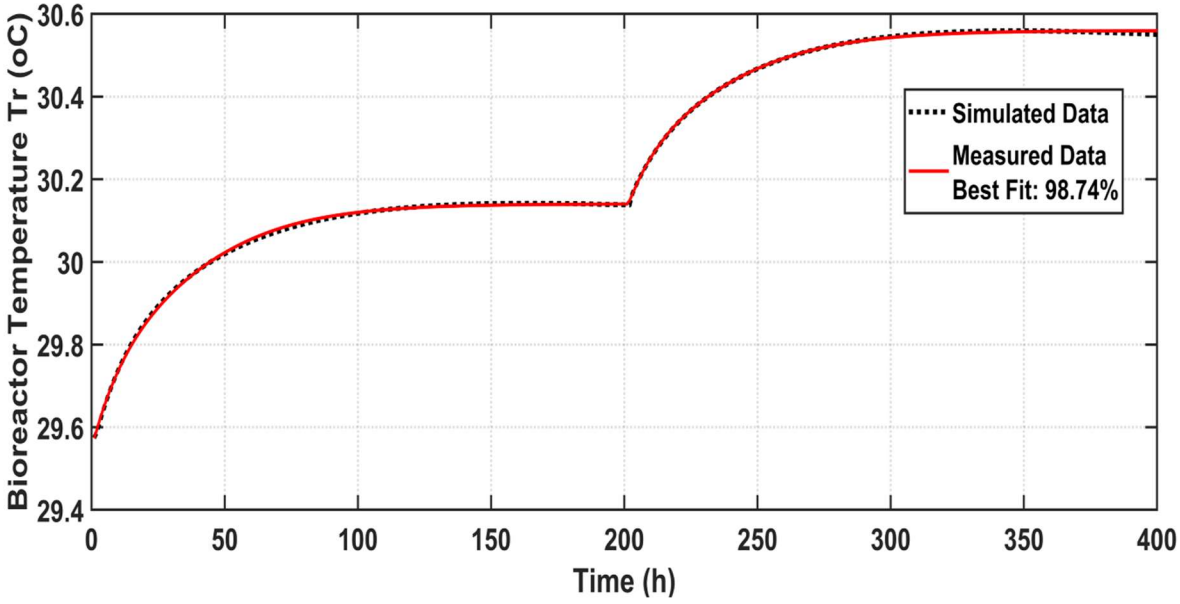

Fig. 3.10 Measured and simulated model output of the nonlinear process model

Figure 3.10 shows the open-loop response of reactor temperature at nominal operating condition and a step change of -5% of input flow rate to the jacket at 200 h. The open-loop response shown in Fig. 3.10 was identified by the Identification tool of MATLAB as shown in Fig. 3.10, and 99% best fit was obtained from simulated data using 4th order state-space model.

$$\dot{X}(t) = AX(t) + B\,u(t) + K\,e(t) \tag{3.18}$$

$$Y(t) = C\,X(t) + D\,u(t) + e(t) \tag{3.19}$$

Where X is the state variable, u denotes the input variable, Y is the output variable and $e(t)$ denote the disturbance. Matrix *A, B, C, D*, and *K* were obtained by identification and model validation of process are as follows:

$$where, A = \begin{bmatrix} -2.078 & -0.02079 & -0.02372 & -0.01896 \\ 0.3587 & -0.04384 & -0.008468 & 0.0007041 \\ 0.4237 & -0.103 & -0.0668 & -0.003852 \\ 0.1479 & -0.001805 & 0.001786 & 0.001182 \end{bmatrix}, B = \begin{bmatrix} -11.54 \\ -2.063 \\ 2.569 \\ 0.8251 \end{bmatrix}$$

$$C = [1.572 \;\; -6.726 \;\; 1.196 \;\; 35.06],\ D = [0],\ K = \begin{bmatrix} 0 \\ 0 \\ 0 \\ 0 \end{bmatrix}$$

The state-space model of Eq. (3.18) and Eq. (3.19) were converted into a 4th order transfer function using MATLAB command $G_p = tf(sys)$, where sys is the state-space model and given by Eq. (3.20)

$$G_p = \frac{-0.0234 \quad ^3 - 0.02055s^2 - 0.001163s + 1.471\times10^{-6}}{s^4 + 2.187s^3 + 0.2497s^2 + 0.004285s + 1.354\times10^{-10}} \tag{3.20}$$

Eq. (3.20) was simplified into pole-zero form using MATLAB command zpk(G_p) and given by Eq. (3.21).

$$G_p = \frac{-0.023469(s+0.8146)(s+0.06094)(s-0.0001262)}{(s+2.067)(s+0.09879)(s+0.02094)(s+3.166\times10^{-5})} \quad (3.21)$$

Since one pole and one zero of Eq. (3.21) is close to the origin, one can cancel out the pole and zero. Therefore, the process model is further simplified to the form of Eq. (3.22).

$$G_p = \frac{-0.023469(s+0.8146)(s+0.06094)}{(s+2.067)(s+0.09879)(s+0.02094)} \quad (3.22)$$

The Eq. (3.22) was further simplified and given by Eq. 3.23.

$$G_p = \frac{-0.27(1.2275s+1)(16.41s+1)}{(0.4837s\quad)(10.1224s\quad)(47.755s+1)} \quad (3.23)$$

The process model given by Eq. (3.23) is a 3rd order and it is challenging to design the PID for this model. Therefore, the process model is reduced to a second-order process by applying some reduction technique given by [46]. According to Rule T2 given by Skogestad [46], the numerator and denominator term given in Eq. (3.23) can be approximated as

$$\frac{(16.41s+1)}{(10.1224s\quad)} \approx 1.6 \quad (3.24)$$

Hence, using Eqs. (3.23) and Eq. (3.24), final approximated transfer function model of bioreactor for temperature control by manipulating the input jacket flow rate is given by Eq. (3.25)

$$G_p = \frac{Tr(s)}{Fj(s)} = \frac{-0.4357(1.2275s\quad)}{(0.4837s\quad)(47.755s+1)} \quad (3.25)$$

Various studies are available in the literature in which different advanced control algorithms have been developed for the reactor temperature control. Since the bioreactor operates in a narrow range of temperature during the fermentation process, an effective control mechanism is required for the tight control of reactor temperature for the optimal growth of microorganisms.

3.2 PID controller design Techniques

3.2.1 PID controller for control of output concentration in CSTR

The PI parameters $Kc\ and\ \tau_I$ were obtained for FOPDT of the TF 2 model given in Eq. (3.4) by applying tuning rules SIMC [46] and Astrom and Hagglund [20]. One more set of PI parameters were obtained using optimization technique with a constraint of 20 % maximum overshoot. Table 3.4 shows different tuning rules along with their corresponding controller parameters. The PI controller calculated using different tuning rules were applied to different forms of CSTR model of second-order linear model Eq. (3.3), nonlinear model, and FOPDT model Eq. (3.4) to control the outlet concentration C_A.

Table 3.4 Different tuning rules for PI controller and their parameters

Process	Tuning Methods	Kc	τ_I(s)	$K_I = \frac{Kc}{\tau_I}$
FOPDT $TF\ 2$	[46]	$\frac{1}{k}\frac{\tau}{\tau_c + \theta}$	$\min(\tau_p, 4(\tau_c + \theta))$	
		0.005	8	0.000628
	[20]	$\frac{0.14}{k} + \frac{0.28\tau}{\theta k}$	$0.33 + \frac{6.8\theta\tau}{10\theta + \tau}$	
		0.00282	7.030	0.000401
$TF\ 1$	Optimal control	0.0028		0.00050

3.2.2 PID controller design for stable SOPDT using direct synthesis (DS) method

In the direct synthesis (DS) approach for controller design, a desired closed-loop response is assumed for set-point change and matched to the closed-loop response [25, 90, 91]. The resulting controller is obtained in terms of a desired closed-loop time constant and process parameters. The time constant of desired response is used as a controller tuning parameter. The main advantage of the direct synthesis approach is that the closed-loop performance requirements set by the control engineer, and it could be incorporated directly through the specification of the desired closed-loop transfer function. The desired closed-loop transfer function can be selected by specifying the closed-loop pole. Therefore, the direct synthesis method is another form of pole placement technique [44, 90].

The DS method does not always provide a controller having PI/PID form. However, by appropriate selection of desired closed-loop transfer function and proper rearrangement of the terms in the resulting controller, it can be converted into the form of PI or PID type controller in case of first and second-order time delay process models. Several process industries viz. chemical, biochemical, and pharmaceutical consist of different process units like distillation unit, heat exchangers, fermenter, and jacketed continuous stirred tank reactor (CSTR) shows second-order transfer function characteristics. Keeping this fact in mind, a second-order plus time delay (SOPDT) model was considered in the present work for the designing of PID controller based on the direct synthesis method. Instead of a double-feedback control structure (Vijayan and Panda [92] and Lee et al. [13]), a single feedback control loop was used in the present study for the synthesis of PID controller. The single feedback control loop is simpler and easy to design. The block diagram of the

proposed feedback loop is shown in Fig. 3.11 in which $G_p(s)$ denotes the plant and $C(s)$ represents the feedback controller PI/PID.

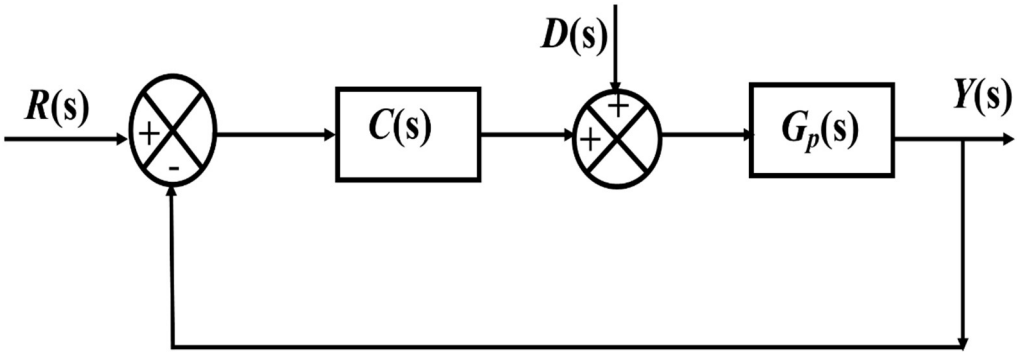

Fig. 3.11 Simple unity feedback control loop

The transfer function of $G_p(s)$ given by Eq. (3.26)

$$G_p = \frac{k_p(fs+g)e^{-\theta s}}{as^2+bs+c} \tag{3.26}$$

Where, the coefficients a, b, c, f *and* g in Eq. (3.26) are constant. The closed-loop response for set-point tracking is given by Eq. (3.27).

$$\frac{Y(S)}{R(S)} = \frac{G_P(S)C(S)}{1+G_P(S)C(S)} \tag{3.27}$$

Chen and Seborg [12] considered a FOPDT model as the desired closed-loop transfer function. However, in the present study, a SOPDT model in Eq. (3.28) was selected as the desired closed-loop transfer function because most of the chemical process units exhibit a second-order plus time delay closed-loop characteristics.

$$\frac{Y(S)}{R(S)} = Q(S) = \frac{e^{-\theta s}}{(\lambda s+1)^2} \tag{3.28}$$

In the above model, λ denotes the tuning parameter for the controller and which was used to calculate the parameters $k_c, \tau_I, and\ \tau_D$. The controller *C*(s) can be obtained by using Eq. (3.27) and Eq. (3.28) moreover, given by Eq. (3.29).

$$C(s) = \frac{1}{G_p}\frac{Q(S)}{1-Q(S)} \tag{3.29}$$

The ideal feedback controller *C*(s) is calculated by using the Eq. (3.26), Eq. (3.28), and Eq. (3.29), as given by Eq. (3.30).

$$C(s) = \frac{as^2+bs+}{kp\,(fs+g)e^{-\theta s}} \times \frac{\frac{e^{-\theta s}}{(\lambda s+1)^2}}{1-\frac{e^{-\theta s}}{(\lambda s+1)^2}} = \frac{as^2+bs+}{kp\,(fs+g)} \times \frac{1}{(\lambda s+1)^2-e^{-\theta s}} \tag{3.30}$$

The delay term $e^{-\theta s}$ in Eq. (3.30) was approximated using Taylor's series expansion as given below:

$$e^{-\theta s} = 1 - \theta s + \frac{\theta^2 s^2}{2!} - \frac{\theta^3 s^3}{3!} + \cdots$$

The delay term up to the 2nd power of 's' was substituted in Eq. (3.30). Furthermore, the resultant expression of the feedback controller *C*(s) was rearranged into the form of Eq. (3.31).

$$C(s) = \frac{1}{s}\left(\frac{(as^2+bs+c)}{k_p\left\{f\left(\lambda^2-\frac{\theta^2}{2}\right)s^2+\left[g\left(\lambda^2-\frac{\theta^2}{2}\right)+f(2\lambda+\theta)\right]s+g(2\lambda+\theta)\right\}}\right) \tag{3.31}$$

The controller expression, as given in Eq. (3.31) is written in a functional form as given by Eq. (3.32) and expression $\varphi(s)$ was obtained by rearranging the terms of Eq. (3.33)

$$C(s) = \frac{\varphi(s)}{s} \tag{3.32}$$

$$\varphi(s) = \left(\frac{(as^2+bs+c)}{k_p\left[f\left(\lambda^2-\frac{\theta^2}{2}\right)s^2+\left\{g\left(\lambda^2-\frac{\theta^2}{2}\right)+f(2\lambda+\theta)\right\}s+g(2\lambda+\theta)\right]} \right) \tag{3.33}$$

The Maclaurin series expansion theorem was used to obtain an ideal form of the PID and controller $C(s)$ given in Eq. (3.34) [61, 92].

$$C(s)=\frac{1}{s}\left(\varphi(0) + \varphi'(0)s + \frac{\varphi"(0)s^2}{2!} + \cdots\right) \tag{3.34}$$

Since the ideal form of PID controller discussed in many control theory books and written as

$$C(s)= k_c\left(1 + \frac{1}{\tau_I s} + \tau_D s\right) \tag{3.35}$$

The controller parameters $k_c, \tau_I \; and \; \tau_D$ were estimated by corresponding coefficients of 's' of Eq. (3.34) and Eq. (3.35). The following expressions for the controller parameters were obtained:

$$k_c = \varphi'(0) \quad \tau_I = \frac{k_c}{\varphi(0)} \quad \text{and} \quad \tau_D = \frac{\varphi"(0)}{2k_c} \tag{3.36}$$

Value of $\varphi(0)$ was calculated by substituting s = 0 in the Eq. (3.33), and first derivative of Eq. (3.33) and then substituting s = 0, one can find the value of $\varphi'(0)$. Similarly, 2nd derivative of Eq. (3.33) and substituting s = 0, $\varphi"(0)$ can be obtained. The values $\varphi(0)$, $\varphi'(0)$ and $\varphi"(0)$ are calculated as follow:

$$\varphi(0) = \frac{N}{D} \tag{3.37}$$

$$\varphi'(0) = \frac{N_1 * D - D_1 * N}{D^2} \tag{3.38}$$

$$\varphi"(0) = \frac{D(N_2 * D - D_2 * N) - 2D_1(N_1 * D - D_1 * N)}{D^3} \tag{3.39}$$

Where, $N = c$; $D = k_p g(2\lambda + \theta)$; $N_1 = b$; $D_1 = k_p\left[g\left(\lambda^2 - \frac{\theta^2}{2}\right) + f(2\lambda + \theta)\right]$; $N_2 = 2a$; $D_2 = k_p f\left(\lambda^2 - \frac{\theta^2}{2}\right)$

Eq. (3.36) to Eq. (3.39) were solved to calculate the PID parameters in terms of λ. The tuning parameter λ was adjusted in such a way that the obtained PID controller provides robust and satisfactory closed-loop results for nominal as well as in case of model uncertainty. The PID controller designed by a direct synthesis approach was applied to several first and second-order time-delay models to evaluate the closed-loop performance. The performance of the PID controller obtained using the present method was compared to other similar tuning rules.

3.2.2.1 Tuning parameter (λ) selection method

The selection of a suitable tuning parameter λ is a challenging and tedious task. The tuning parameter is selected in such a way that the obtained controller should provide robust performance with a minimum integral error. A small value of λ gives a quick response and shows a better result in the case of load change for stable processes, whereas a high value of λ provides stability and robustness of the controller. To select the optimum value of λ, an approach based on Maximum sensitivity *Ms* was applied. In this approach, *Ms* was considered as performance index and defined as $Ms = max\left|\frac{1}{[1+G_p G_c(i\omega)]}\right|$. Graphically *Ms* is the inverse of the smallest distance from the Nyquist curve to the critical point (−1, 0) in the Nyquist plot. *Ms* value can also be used to choose a range for the gain margin (GM) and phase margin (PM). Veldsink, et al. [93] and Skogestad and Postlethwaite [94] gave the

following relations to estimate the range of GM and PM in terms of *Ms* as given by Eq. (3.40).

$$\text{GM} \geq \frac{M_s}{M_s-1};\ \text{PM} \geq\ 2sin^{-1}\left(\frac{1}{2M_s}\right) \tag{3.40}$$

The lower bound of GM and PM decreases as *Ms* increases. The minimum value of GM is 1.7, and 35 degrees has been recommended for PM for typical stable processes. There are certain limitations of the controller for controlling process and to achieve the desired robust closed-loop response [22]. In the present study, the tuning parameter was selected to achieve maximum sensitivity (*Ms*) value in the range of 1.2-1.8 because the controller within this range of *Ms* value provides robust and better-closed loop performance.

3.2.3 Internal Model Control (IMC) Technique

A brief description of the internal model control (IMC) technique has already been discussed in literature review section of the thesis. The IMC design has an interesting application for designing Q-parameterized controllers, which provide satisfactory results for both fundamental and practical applications. The concept behind evolution of IMC is shown in Fig. 3.12 A and Fig. 3.12 B represents the IMC structure.

The closed-loop response *Y*(s) for the IMC structure shown in Fig. (3.12 B) is given by Eq. (3.41). This equation can also be written in the form of sensitivity function S(s) and complementary sensitivity function T(s) as given by Eq. (3.42).

$$Y(s) = \frac{G_pQ}{1+Q(G_p-G_m)}R + \frac{1-G_mQ}{1+Q(G_p-G_m)}D \tag{3.41}$$

Therefore,
$$Y(s) = T(s)R(s) + S(s)D(s) \tag{3.42}$$

For the perfect model, i.e., there is no plant/model mismatch ($G_p = G_m$), these functions can be simplified to

$$T(s) = G_m Q;\ S(s) = 1 - T(s) = 1 - G_m Q; \text{ and } Q = G_m^{-1} T(s) \tag{3.43}$$

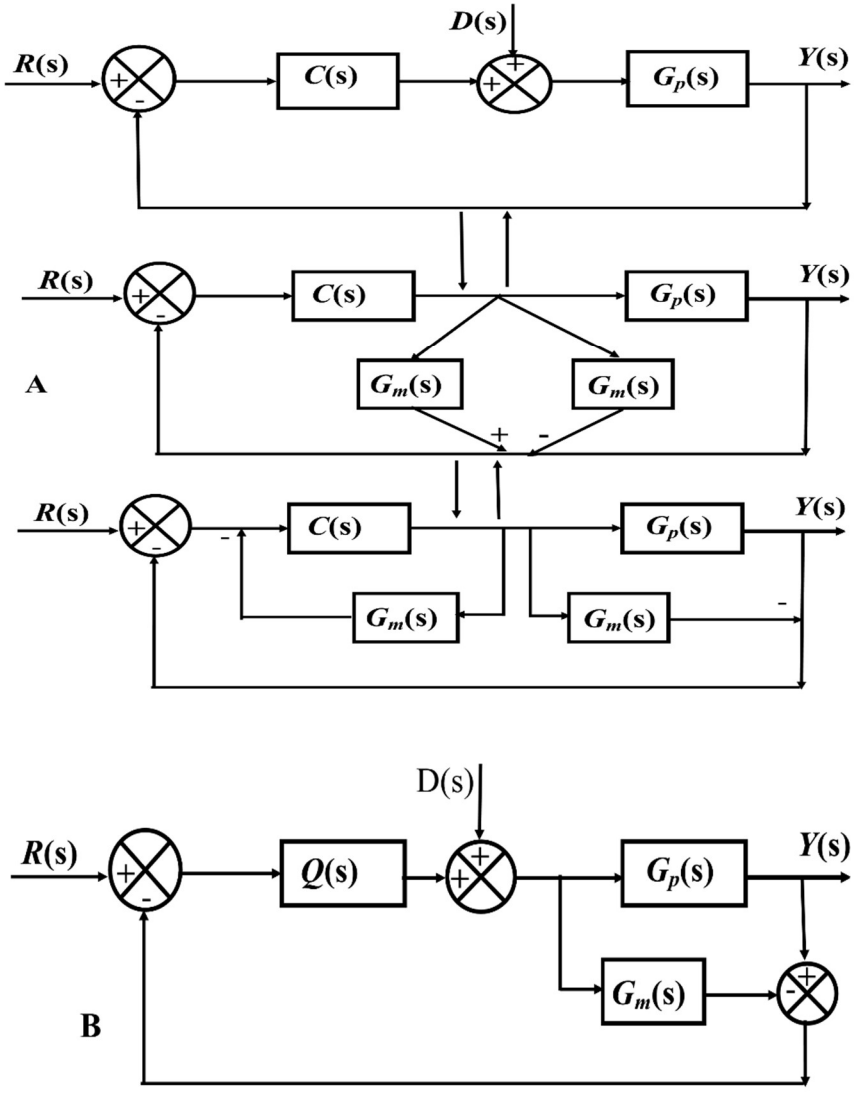

Fig. 3.12 (A) Evolution of IMC Controller (B) IMC control structure

The feedback control loop shown in Fig. 3.12 (A) is obtained by simplification of IMC control loop shown in Fig. 3.12 (B) and rearranging the IMC controller Q(s) to the feedback controller C(s) as given by Eq. (3.44). Further, the resulting controller may not necessarily in a standard form of PID controller. However, it can be simplified to a PI/PID controller or PID with a lead-lag filter in series by some simplification and rearrangement. The designed PID should be stable, simple in structure, robust in nature, easy to understand, and implementable on the real system. The IMC structure provides a suitable framework for satisfying these objectives.

$$C(s) = \frac{Q(s)}{1-G_m(s)Q(s)} \tag{3.44 a}$$

$$Q(s) = \frac{C(s)}{1+G_m C(s)} \tag{3.44 b}$$

3.2.3.1 IMC filter selection

The IMC controller is augmented with a filter $f(s)$ to make the controller proper, realizable, and internally stable. The filter structure and parameter both are selected in such a way that it provides an optimal compromise between performance and robustness of the controller. Morari and Zafiriou [24] suggested a detail selection procedure for the IMC filter. To simplify the design task, the filter structure is fixed, and then a search made over a small number of filter parameters to obtain desired robustness characteristics. It is logical to choose f such that the closed-loop system retains its asymptotic tracking properties (Type m). For the system of Type m, f has to satisfy

$$\lim_{s\to 0} \frac{d^k}{ds^k}\left(1 - G_m \tilde{Q} f\right) = 0 \qquad 0\leq k<m \tag{3.45}$$

If G_m is designed to satisfy Eq. (3.45) for f=1 then the conditions on f for Eq. (3.45) to be satisfied as

$$\lim_{s\to 0}\frac{d^k}{ds^k}(1-f)=0 \qquad 0\leq k<m \tag{3.46}$$

Thus

Type 1: $$f(0)=1 \tag{3.47}$$

Type 2: $$f(0)=1 \; and \; \lim_{s\to 0}\frac{df}{ds}=0 \tag{3.48}$$

Typically, one can use one parameter filters with unity steady-state gain of the form

$$f=(\beta_{m-1}s^{m-1}+\cdots\beta_1 s^1+1)\frac{1}{(\lambda s+1)^n} \tag{3.49}$$

Where λ is an adjustable filter parameter, and n is selected large enough to make Q proper and β_i is chosen to satisfy Eq. (3.46). The simplest filters of the form Eq. (3.50) and Eq. (3.51) which satisfies Eq. (3.46) are

Type 1 $$f=\frac{1}{(\lambda s+\ )^n} \tag{3.50}$$

Type 2 $$f=\frac{(n\lambda s+1)}{(\lambda s+1)^n} \tag{3.51}$$

3.2.3.2 PID controller design for USOPDT using IMC technique

In present work, an IMC based PID controller design approach is discussed for unstable second-order time-delay (USOPDT) system with right hand of the complex plane (RHP) zero in numerator. Internal Model Control (IMC) system shown in Fig. 3.13 (A) and their

equivalent feedback control loop is shown in Fig. 3.13 (B) were considered for designing of IMC-PID controller for unstable second-order time-delay process.

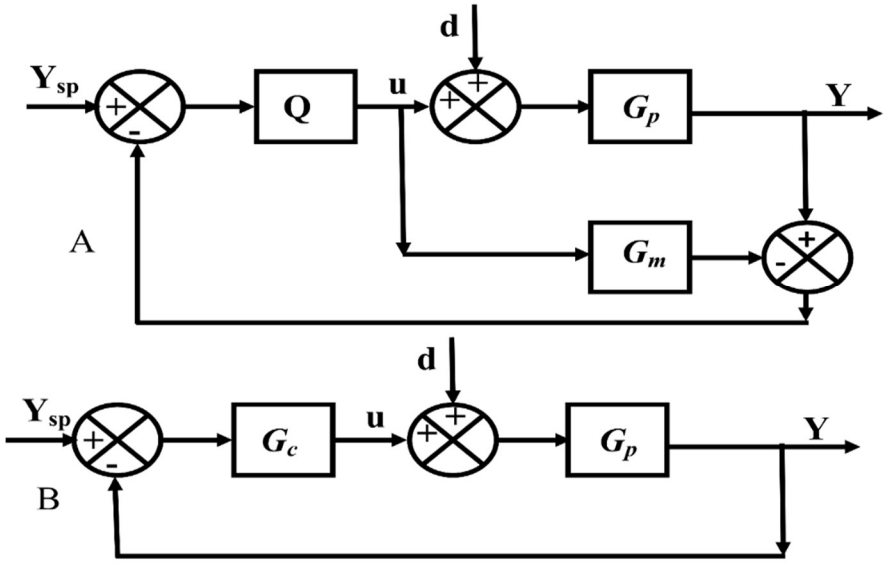

Fig. 3.13 (A) Internal Model Control (IMC) structure (B) Feedback control system

In the figures $G_p$represents the process transfer function and G_m depicted as the process model. The IMC controller is denoted by Q(s) and $G_c$represents its equivalent feedback controller.

Design procedure of the IMC controller is a two-steps approach (i) Nominal Performance: IMC controller $\tilde{Q}$ is selected to provide good system response in case of a perfect model or in the absence of model uncertainty and (ii) the IMC controller $\tilde{Q}$ is augmented by a low pass filter f (Q=$\tilde{Q}f$) to make the controller proper and realizable and which provides robust performance and robust stability. This method can specify the sensitivity S(s) and complementary sensitivity T(s) functions and specify the closed-loop response natures.

The IMC design includes mainly two steps. The first step ensures that Q is stable and causal; the second step requires Q to be proper.

Step 1: The process model G_m is factored into two part of $G_{m+}G_{m-}$.

G_{m+} represents the nonminimum phase part of the process model, a is all Right-Half-plane (RHP) zero and time delays. However, G_{m-} denotes the minimum phase part of the process model and invertible; an IMC controller is defined as

$$\tilde{Q} = G_{m-}^{-1}$$

is stable and causal.

The factorization of G_{m+} from G_m is dependent upon the objective function chosen [24].

*Step 2:*The IMC controller $\tilde{Q}$ is augmented with a filter *f*(s) so that the controller becomes proper and causal and obtained final IMC controller in the form of $Q = \tilde{Q}f(s)$.

As discussed earlier in the chemical, biochemical, pharmaceutical, etc. industries, several process units exhibit characteristics of unstable second-order plus time delay during their operation. Different forms of the second-order time-delay system derived from the process industries may be in the forms of transfer function model given in Eq. (3.52 a) - Eq. (3.52 d).

$$G_p = \frac{k_p e^{-\theta}}{(\tau_1 s+1)(\tau_2 s-1)} \quad (3.52\text{ a})$$

$$G_p = \frac{k_p e^{-\theta s}}{(\tau_1 s-1)(\tau_2 s-1)} \quad (3.52\text{ b})$$

$$G_p = \frac{k_p e^{-\theta s}}{s(\tau s - 1)} \quad (3.52\ c)$$

$$G_p = \frac{k_p(1 \pm ps)e^{-\theta s}}{(\tau_1 s \pm 1)(\tau_2 s - 1)} \quad (3.52\ d)$$

Due to the presence of RHP pole and zero, the model in Eq. (3.52 d) is more difficult to control. Therefore, a general transfer function model of Eq. (3.53) was taken as the process transfer function for the design of proposed IMC-PID controller.

$$G_p = \frac{K_p(1 - ps)e^{-\theta s}}{a_1 s^2 + a_2 s + 1} \quad (3.53)$$

Where $a_1 > 0,\ a_2 < 0$ and RHP pole of G_p may be real or complex. According to the IMC principle, the controlled variable in the IMC-structure given in Fig. (3.13A) is given as

$$Y = \frac{G_p Q}{1 + Q(G_p - G_m)} Y_{sp} + \left[\frac{1 - Q G_m}{1 + Q(G_p - G_m)}\right] d \quad (3.54)$$

For the nominal case i.e. $G_p = G_m$, the set-point and disturbance response can be written as:

$$Y = G_p Q Y_{sp} + (1 - Q G_m) d \quad (3.55)$$

The process model G_m is factored into two parts as $G_m = G_{m+} G_{m-}$ to design the IMC controller. G_{m+} denotes noninvertible part which includes time delay and RHP zero of the process model and G_{m-} describes the invertible parts of the model. Therefore, the model is decomposed as:

$$G_{m-} = \frac{K_p}{a_1 s^2 + a_2 s + 1} \text{ and } G_{m+} = (1 - ps)e^{-\theta} \quad (3.56)$$

In the present work, a fourth-order filter $f(s)$ as given by Eq. (3.57) is selected as the IMC filter for the designing of IMC-PID controller for an unstable second-order time-delay process. The proposed filter was also used by several other researchers [19, 28, 47, 62, 64].

$$f(s) = \frac{\beta_2 s^2+\beta_1 s+1}{(\lambda s+1)^4} \tag{3.57}$$

After solving Eq. 3.56 and Eq. 3.57, IMC controller Q was calculated and given by Eq. (3.58).

$$Q = \tilde{Q} f(s) = \frac{a_1 s^2+a_2 s+1}{K_p} \times \frac{\beta_2 s^2+\beta_1 s+1}{(\lambda s+1)^4} \tag{3.58}$$

The equivalent feedback controller $C(s)$ of IMC controller given in Eq. (3.58) was estimated by Eq. (3.59).

$$G_c(s) = \frac{Q}{(1-QG_p)} = \frac{(a_1 s^2+a_2 s+1)(\beta_2 s^2+\beta_1 s+1)}{K_p[(\lambda s+1)^4-(1-ps)(\beta_2 s^2+\beta_1 s+1)e^{-\theta s}]} \tag{3.59}$$

The feedback controller $G_c(s)$ mentioned in Eq. (3.59) is not in a standard form of PID, and therefore, this equation can be simplified and rearranged in the form of PID. The time delay term $e^{-\theta s}$ in Eq. (3.59) can be approximated by Taylor series theorem as $e^{-\theta s} = 1 - \theta s$ and final form of the feedback controller given in Eq. (3.60).

$$G_c(s) = \frac{(a_1 s^2+a_2 s+1)(\beta_2 s^2+\beta_1 s+1)}{K_p[(\lambda s+1)^4-(1-ps)(\beta_2 s^2+\beta_1 s+1)(1-\theta s)]} \tag{3.60}$$

Further, Eq. (3.60) was rearranged in the form of Eq. (3.61) and which can be further rearranged to PID form,

$$G_c(s) = \frac{(a_1 s^2+a_2 s+1)(\beta_2 s^2+\beta_1 s+1)}{K_p(4\lambda-\beta_1+\theta+p)s[x_1 s^3+x_2 s^2+x_3 s+1]} = \frac{(a_1 s^2+a_2 s+1)(\beta_2 s^2+\beta_1 s+1)}{K_p hs[x_1 s^3+x_2 s^2+x_3 s+1]} \tag{3.61}$$

Where,

$$h = (4\lambda - \beta_1 + \theta + p) \quad (3.62\ a)$$

$$x_1 = (\lambda^4 - p\theta\beta_2)/h \quad (3.62\ b)$$

$$x_2 = (4\lambda^3 - p\theta\beta_1 + \theta\beta_2 + p\beta_2)/h \quad (3.62\ c)$$

$$x_3 = (6\lambda^2 - \beta_2 - \theta p + p\beta_1 + \theta\beta_1)/h \quad (3.62\ d)$$

The denominator term of Eq. (3.61) is factorized to obtain the coefficients x_1, x_2 and x_3 as given by Eq. (3.63).

$$x_1 s^3 + x_2 s^2 + x_3 s + 1 = (\gamma s + 1)(a_1 s^2 + a_2 s + 1) \quad (3.63)$$

The coefficients x_1, x_2 and x_3 were calculated by equating the corresponding coefficients of equal order of's' in Eq. (3.63).

$$x_1 = \gamma a_1 \quad (3.64\ a)$$

$$x_2 = \gamma a_2 + a_1 \quad (3.64\ b)$$

$$x_3 = \gamma + a_2 \quad (3.64\ c)$$

The coefficients β_1, β_2 and γ were calculated by solving Eq. (3.62) and Eq. (3.64), and given by Equations 3.65 a, 3.65 b, and 3.65 c.

$$\beta_1 = \frac{y_4 z_1 - y_2 z_2}{y_1 y_4 - y_2 y_3} \quad (3.65\ a)$$

$$\beta_2 = \frac{\beta_1 y_1 - z_1}{y_2} \quad (3.65\ b)$$

$$\gamma = \frac{x_1}{a_1} \tag{3.65 c}$$

where,

$$y_1 = a_1 p\theta - {a_1}^2 \tag{3.66 a}$$

$$y_2 = a_2 p\theta + a_1(p + \theta) \tag{3.66 b}$$

$$y_3 = a_1(p + \theta) + a_1 a_2 \tag{3.66 c}$$

$$y_4 = a_1 - p\theta \tag{3.66 d}$$

$$z_1 = 4a_1\lambda^3 - a_2\lambda^4 - {a_1}^2(4\lambda + \theta + p) \tag{3.66 e}$$

$$z_2 = \lambda^4 + a_1 a_2(4\lambda + \theta + p) - a_1(6\lambda^2 - p\theta) \tag{3.66 f}$$

Using the above steps the feedback controller $G_c(s)$ was simplified to a standard form of PID and given by Eq. (3.67) similar approach was given by [95] to simplify the controller into PID form.

$$G_c(s) = K_c\left(1 + \frac{1}{\tau_I s} + \tau_D s\right)\frac{1}{\alpha s+1} \tag{3.67}$$

Where, $K_c = \frac{\beta_1}{K_p h}$, $\tau_I = \beta_1$, and $\tau_D = \frac{\beta_2}{\beta_1}$ and $\alpha = \gamma = \frac{x_1}{a_1}$ and λ is the tuning parameter of the controller. The controller parameters depend on the tuning parameter of λ, and the desired closed-loop performance and robustness can be achieved by adjusting the value of λ.

The proposed IMC-PID applied to different forms of unstable and integrating second-order time-delayed (SOPDT) with or without RHP zero in the numerator. This method also applied for temperature control of bioreactors in the fermentation process for ethanol

production. The performance of the controller was evaluated in terms of ITAE and TV value. Robustness of controller was calculated by introducing of 10-20 % perturbations into various process parameters.

3.2.3.3 Selection guideline for λ

The controller tuning parameter λ is adjusted in such a manner that provides desired performance and robustness of the proposed controller. There is always a possibility of trade-off between performance and robustness of a controller. For a stable process, faster response in case of set-point tracking and disturbance rejection is obtained for a small value of λ. However, it is not always correct for unstable processes. The performance may be improved by taking optimum value of λ which provides more stable and robust performance for unstable process. The selection guidelines of the tuning parameter λ have been suggested by several researchers. A simple method of λ selection guideline based on peak of maximum sensitivity *Ms* is discussed in [61, 62, 96]. The present study also considered a similar approach to λ selection. In this approach a plot of *Ms* versus λ was drawn for a particular transfer function model. In the plot of *Ms* vs λ, a peak value of *Ms* was obtained some where of the plot at a particular value of λ and after that decreases quickly and finally becomes constant up to a specific range of λ. Generally, λ is selected after the peak of *Ms,* and the corresponding controller parameters are evaluated to achieve the desired performance and robustness. A similar selection method was used in the various other recently published papers [19, 22, 61, 96].

3.2.3.4 Robustness and Stability Analysis

The stability and performance or guarantee for the robustness of the closed-loop system is an important aspect of the control system design. The possibility of plant/model mismatch, i.e. model uncertainty always exists in the process industries. The plant/model mismatch may occur in the industries due to linearization of nonlinear process, reduction of higher-order model to lower-order approximated model, or the presence of uncertainty in process input/output parameters. In present work, only the parametric uncertainties are considered, and a particular value of perturbation was introduced into the process parameters such as in gain K_p, dead time θ and in time constants τ_1 and τ_2. For a robust and stable feedback system, the following condition must be satisfied [24].

$$\|l_m(j\omega)T(j\omega)\| < 1 \; \forall\omega \in (-\infty, \infty) \tag{3.68}$$

Where $T(s = j\omega)$ denotes the complementary sensitivity function and which is defined as $T(s) = C(s)G_p(s)/(1 + C(s)G_p(s))$ and $l_m(s = j\omega)$ is multiplicative uncertainty bound on the process model. The multiplicative uncertainty in the process model can be stated as

$$l_m(j\omega) = \left|\frac{G_p(j\omega) - G_m(j\omega)}{G_m(j\omega)}\right| \tag{3.69}$$

If the uncertainty present in time delay of the process, λ should be selected so that the following condition is satisfied

$$\|T(j\omega)\|_\infty < \frac{1}{|e^{-\Delta\theta s} - 1|} \tag{3.70}$$

If it appeared in the process gain, the parameter λ should fulfill the following condition.

$$\|T(j\omega)\|_\infty < \frac{1}{|\Delta K_p|/K_p} \tag{3.71}$$

The sensitivity must fulfill the constraints, and complementary sensitivity functions are provided in the following Eq. (3.72) to obtain the desired robustness of the process [24].

$$\|l_m(j\omega)T(j\omega) + w_m(j\omega)(1 - T(j\omega)\| < 1 \tag{3.72}$$

where, $w_m(j\omega)$ is *Ms* uncertainty bound which is $(1 - T(j\omega))$. Therefore, λ must be selected in such a way that the resulting controller satisfies the robust performance and stability limitations.

3.2.3.5 Performance measurement

The performance of the controller in case of each problem is calculated in terms of conventional parameters such as % overshoot, rise time, etc. More quantitative and reliable performance parameters such as integral of time-weighted absolute error (ITAE) and the control action, i.e., total variation (TV) are also calculated. The close-loop results of the proposed method were compared to different similar tuning rules based on designing of IMC-PID using *Ms* approach. A brief overview of performance parameters used in present study are as follows:

Overshoot (%OS)

Overshoot is a measure of how much the closed-loop response exceeds the ultimate value following a step change in setpoint or disturbance. Overshoot is calculated in terms of percentage and denoted by %OS.

Rise time (t_r)

It indicates the speed of the response, and it is the time needed to reach the first time to ultimate value or set point.

Settling time (t_s)

It is the time required to reach the final steady-state value or ultimate value for set-point or disturbance change.

Time integral error indices

The performance of the controller indicated by the various time integral error indices like integral of the absolute error (IAE), integral of the square error (ISE) and integral of the time-weighted absolute error (ITAE).

$$IAE = \int_0^\infty |e(t)|dt$$

$$ISE = \int_0^\infty e(t)^2 dt$$

$$ITAE = \int_0^\infty t|e(t)|dt$$

Where $e(t)$ represents the error between the set-point and the measurement. ITAE criterion penalizes the long-term errors whereas the ISE penalizes larger error. The IAE criterion provides controller settings that are between those for the ITAE and ISE criteria.

Total variation

Total variation (TV) measures the control efforts (manipulated input usage) or smoothness of the control signal. Therefore, the performance of the controller can also be given by

parameter TV [46]. If control signal $u(t)$is discretized as $[u_1, u_2, u_3 \ldots u_i \ldots]$, then $TV = \sum_{i=1}^{\infty}|u_{i+1} - u_i|$ should be minimum.

Set-point weighting

The ideal form of PID discussed in the various control theory books can be written as:

$$C(s) = K_c\left(1 + \frac{1}{\tau_i s} + \tau_D s\right)$$

An undesirable overshoot is observed in many cases of closed-loop response. Different researchers used various technique viz. a set-point filter or set-point weighting parameter to remove the undesirable overshoot. A set-point weighting method suggested by Åström and Hägglund [44] is the most widely accepted control structure given in Eq. (3.73) is used to deal with undesirable overshoot.

$$u(t) = K_c\left([br(t) - y(t)] + \frac{1}{\tau_I}\int_0^t [r(t) - y(t)]d\tau + \tau_D \frac{d[cr(t) - y(t)]}{dt}\right) \qquad (3.73)$$

Where 'b' denotes the weighting parameter of set-point, and c denotes the weight for the derivative time constant of the controller. These parameters are chosen between 0 to 1. The setpoint weighting parameter 'b' is applied to minimize undesirable overshoot by selecting it's value between 0.2 to 0.5 as given by the researchers to minimize the overshoot. A similar range of setpoint weighting parameter 'b' was proposed for integrating or unstable processes[97]